The size effect of crystalline inclusions on the fracture modes in glass–ceramic materials

2007 J. Phys.: Condens. Matter 19 266209

(http://iopscience.iop.org/0953-8984/19/26/266209)

IOP PUBLISHING JOURNAL OF PHYSICS: CONDENSED MATTER

J. Phys.: Condens. Matter **19** (2007) 266209 (12pp) doi:10.1088/0953-8984/19/26/266209

The size effect of crystalline inclusions on the fracture modes in glass–ceramic materials

C A Charitidis[1,4], T E Karakasidis[2], P Kavouras[3] and Th Karakostas[3]

[1] School of Chemical Engineering, National Technical University of Athens, 9 Heroon, Polytechniou street, Zografos, GR-157 80 Athens, Greece
[2] Department of Civil Engineering, University of Thessaly, Pedion Areos, GR-38834 Volos, Greece
[3] Department of Physics, Solid State Section, Aristotle University of Thessaloniki, GR-54124 Thessaloniki, Greece

E-mail: charitidis@chemeng.ntua.gr

Received 13 November 2006, in final form 8 May 2007
Published 7 June 2007
Online at stacks.iop.org/JPhysCM/19/266209

Abstract

The main parameters influencing the mechanical performance of glass–ceramic materials are the shape and mean size of the ceramic phase, i.e. the crystalline inclusions. The aim of the present work is twofold: first, to study the effect of the above parameters on the modes of fracture in two kinds of glass–ceramic materials by the use of the static microindentation technique; second, to interpret the experimental results by the application of a simple physical model. It was found that reduction in the size of granularly shaped crystallite inclusions or reduction of the width of needle-like crystalline inclusions results in an increase of the extent of crack propagation, while the fracture mode shifts from intergranular to transgranular. These observations were successfully interpreted in terms of energetic arguments related to the size of the crystalline inclusions with respect to the width of a disordered zone acting as an interface between them and the amorphous matrix.

1. Introduction

It is a common practice for the ceramic industry to modify the coherence of grain boundaries in order to control the active fracture modes in ceramic products [1–3], in other words to decide whether the cracks should propagate in transgranular or intergranular mode. In the former case the crack paves its way irrespectively of the direction of the grain boundaries, i.e. the interfaces between the different phases. In the latter case the crack preferentially follows them, i.e. debonds the interfaces [4]. It is now widely accepted that intergranular fracture is connected to high toughness, while transgranular to high strength [5]. These fracture modes have been

[4] Author to whom any correspondence should be addressed.

extensively studied in the case of ceramic materials, while they have not received the same attention in the case of glass–ceramic materials.

It is reported in the literature the increased strength of a machinable bioactive glass–ceramic, where the composition and morphology of the separated crystal phases promote transgranular fracture [6]. Tailoring the composition of a surface crystalline layer [7] and modification of the crystal volume fraction [8] for the increase of the fracture toughness are also reported in the literature. Relatively more studies are concerned with the study of fibre reinforced composite materials with glass–ceramic matrices, the so-called brittle matrix composites. In these studies special attention is given on the nature of the fibre/matrix interfaces and the effect they have on the fracture modes and failure mechanisms [9, 10]. In a work of Boccaccini *et al* [11] the significant strength reduction, due to the oxidative degradation of carbon rich layer in the fibre/matrix interface, is highlighted. The crack deflection at the fibre/matrix interfaces is connected with the need for poor bonding in the cases where high toughness is needed [12].

In the present study the influence of crystalline inclusions size on the mechanical properties of two types of glass–ceramic products has been investigated. The mechanical properties that will be studied are the modes of fracture of the glass–ceramic materials and a simple physical model will be applied in order to interpret the results. One glass–ceramic type contains granularly shaped and the other contains randomly oriented needle-like crystalline inclusions. The strength and toughness of glass–ceramic materials depends on their morphological and microstructural features that can be tailored in order to affect the mechanical performance of glass–ceramic end-products. It has also been reported that understanding the fracture mechanisms can glean light into the inter-relations with wear that is critical to the prevention of catastrophic failure [13].

The properties that can be tailored are the composition, shape and mean size of the crystalline inclusions. A detailed description of the procedure and tailoring process has been presented elsewhere [14]. Devitrifying the same starting vitreous product can result in glass–ceramic products containing crystalline inclusions of different compositions. This can be achieved by changing the temperature of thermal treatment. Their shape can be tuned by changing the mode of crystallization between surface and bulk [15]. Additionally, glass–ceramic materials with different morphologies can be obtained by changing the heat treatment scenario. Application of the one-stage petrurgic scenario, which is composed of prolonged cooling, will result in relatively high population densities and large separated crystallites [16]. Since their composition, shape and mean size are the most easily tuned properties, they will be referred to as the functional properties. As mentioned above, in the present work the effect of crystalline inclusions size on the mechanical properties has been studied.

2. Experimental details

Glass–ceramic samples were produced by one-stage isothermal treatment of the parent glasses, i.e. the temperature was risen up to 900 °C and remained constant for 60 min. The batch compositions of the parent glasses are listed in table 1. All starting materials were in oxide form. After weighting, all batch components were milled together in a Fritsch Pulverisette 'O' vertically vibrating ball milling apparatus, in order to obtain a homogeneous solid mixture. This mixture was put in a platinum crucible and all batch components were subsequently co-melted in a Nabertherm high temperature electric furnace in air for 2 h at a temperature of 1400 °C. Visual inspection during the melting process revealed that both batch compositions melted at the temperature interval between 700 and 750 °C. The homogenized melts were poured on a stainless steel plate and quenched in the form of solid droplets.

Table 1. A list of the batch compositions of the parent vitreous products, the annealing conditions and the resulting glass–ceramic products.

Code name	Composition (wt%)				Annealing		Ceramic phase	
	Fe_2O_3	PbO	SiO_2	Na_2O	T (°C)	t (min)	Composition	Shape
G	30	20	35	15	900	60	$Pb_8Fe_2O_{11}$	Granular
N	36	24	25	15	900	60	Fe_2O_3	Needle

The as-quenched products were single phase elementally homogeneous glasses. Their vitreous nature was revealed by the fact that the respecting differential scanning analysis thermographs possessed the characteristic glass transition temperature (T_g) endotherm. The position of the T_g of G and N products was found approximately at 430 °C [17]. The elemental homogeneity was found by energy dispersive spectrometry (EDS) analysis. A number of 20 EDS analyses for the constituent elements, namely Fe, Pb, Si and Na, were obtained for every product. The composition variation of these elements was comparable to the accuracy of the method, namely ±1 at.%. Transmission electron microscopy studies made of the vitreous matrices revealed featureless areas in bright view images with corresponding electron diffraction patterns that had the form of a diffused halo, characteristic of amorphous matter [17].

The shape of the crystalline inclusions was determined by the batch composition of the parent vitreous product (table 1). Glass–ceramic product G contained granularly shaped crystalline inclusions of various sizes. However, there were areas with similar sizes, as will be shown in the results part. Consequently, the microindentations as well as the induced cracks propagated in areas with crystalline inclusions of similar sizes. In the case of N product the above aspects were not an issue, since the interaction of a propagating crack with one needle crystalline inclusion is the most interesting aspect for the present study. Thermal treatment conditions, as well as the morphology and the composition of the crystalline inclusions are listed in table 1.

The modes of fracture were determined by observing the paths of crack propagation with respect to the crystallite/amorphous matrix interfaces by optical microscopy. Scanning electron microscopy observations were also performed, but the crack path obtained was not as clear as in the case of the optical measurements, mainly due to the poor contrast between the crack and the residual amorphous matrix. Cracks were produced on mechanically polished flat surfaces of the thermally treated products with a Vickers diamond indenter. An Anton-Paar MHT-10 microhardness tester was utilized [18] attached on a Zeiss Axiolab-A optical microscope. The indentation parameters were set at: load = 1–3 N, duration = 10 s and loading slope = 0.2 N s^{-1}. The duration of 10 s is a typical time that is long enough for the onset of plasticity, while the load range was selected in order to produce indentations with clearly defined radial cracks.

The results were interpreted by applying a simple mathematical model based on energetic arguments related to the size of the crystalline inclusions with respect to the width of a disordered zone acting as an interface between them and the amorphous matrix.

3. Results

Two types of glass ceramics were studied. The first type was composed of granularly shaped crystalline inclusions embedded in a vitreous matrix. Figures 1(a) and (b) depict two optical micrographs obtained from G glass–ceramic product under the same magnification

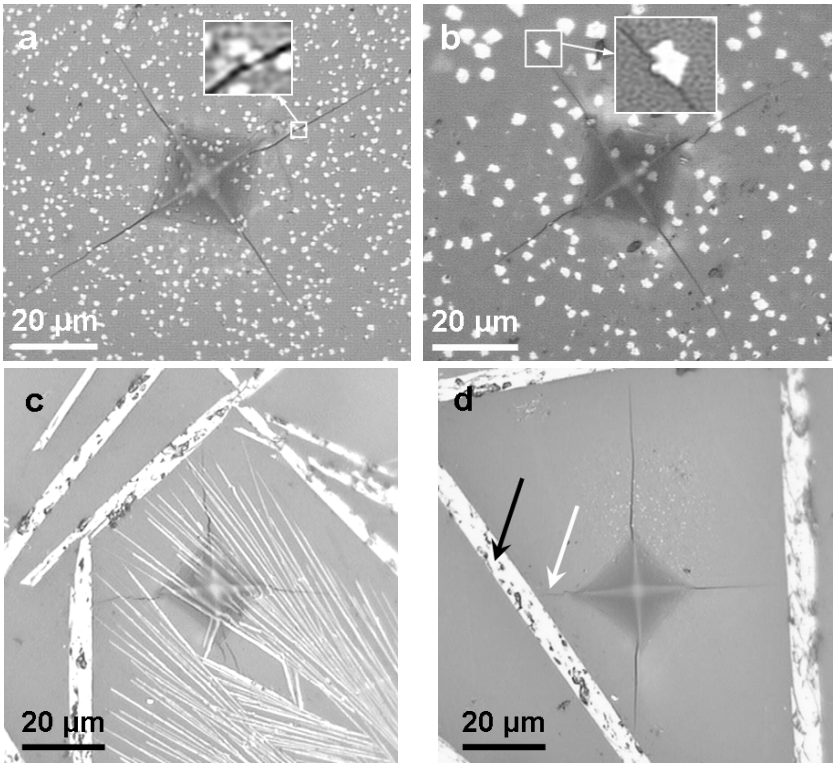

Figure 1. Optical micrographs of indentation-induced radial cracks from G and N products indicating transgranular ((a) and (c)) and intergranular ((b) and (d)) propagation. Enlarged photos showing transgranular and intergranular fracture events are shown as insets in figures (a) and (b), respectively.

for comparison reasons. The difference in the mean crystalline inclusion size and the way that the indentation-induced radial cracks propagate can be observed. When the mean crystalline inclusion size is 0.5 μm crack propagation occurs in straight lines (figure 1(a)) irrespectively of the position of the interfaces. In this case, relatively small $Pb_8Fe_2O_{11}$ crystalline inclusions are traversed from the crack. As a result, in this case the fracture mode is mainly transgranular. When the mean crystalline inclusion size is 3 μm the indentation-induced radial cracks propagate in curved paths (figure 1(b)). In this case, the relatively larger crystalline inclusions cannot be traversed by the propagating crack. The cracks are deflected from the crystalline inclusion/amorphous matrix interfaces and consequently the fracture mode is mainly intergranular. Transgranular modes can also be found but they are considerably less than intergranular ones. As a result, it can be assumed that the increase in the mean size is the reason for the shift of the fracture mode from transgranular to intergranular.

The volume fraction of crystalline inclusions in the case of G glass–ceramic product depends on their mean size. Qualitatively, it was observed that the volume fraction of the crystalline inclusions is inversely proportional to their mean size. Our calculations revealed that in the case of the smaller crystalline inclusions with mean size of 0.5 μm the volume fraction reaches 14%. In the case of the larger crystalline inclusions with mean size close to 8 μm the volume fraction is approximately 7%. In the case of N glass–ceramic products the trend in the volume fraction with respect to the width of the crystalline needles is qualitatively

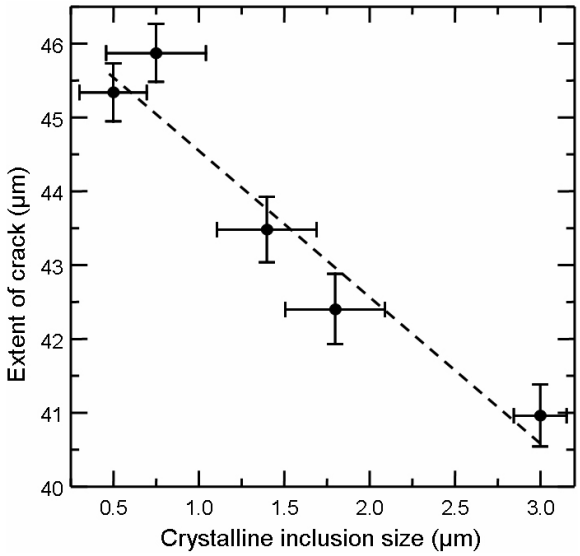

Figure 2. The extent of crack propagation as a function of mean size of $Pb_8Fe_2O_{11}$ crystalline inclusions for both transgranular and intergranular fracture modes.

the same. The only difference is in the absolute values of the volume fraction. In the case of the thinner crystalline needles with mean width of 0.5 μm the volume fraction reaches 30%. In the case of the thicker crystalline needles with mean width close to 8 μm the volume fraction is approximately 11%.

In figure 2 the extent of crack is plotted as a function of mean crystallite size. In this point, the extent (or effective distance) of a crack is defined as follows: it is the length of the straight line that connects the corner of the Vickers indentation print, from where the crack has emanated, with the crack tip. All indentations were made on different areas of G glass–ceramic product that is composed of granularly shaped $Pb_8Fe_2O_{11}$ crystalline inclusions. It is shown quantitatively that the increase of the mean crystallite size causes the reduction in the extent of crack propagation. The error bars represent the standard deviations since each point represents ten measurements. For the smaller crystallite sizes the radial cracks propagate in straight lines, i.e. transgranularly, and the extent of propagation is increased with respect to larger crystallite sizes where the mode of fracture is intergranular. For larger crystallite sizes the crack will not follow a straight line when it meets the large crystallites and thus it will travel a shorter effective distance although that the length of the crack itself may be longer.

N glass–ceramic product contains needle-shaped haematite (Fe_2O_3) randomly oriented crystalline inclusions. In this case it was found that the width of the crystalline needles determines the mode of fracture. In N product, the cracks cut through the crystalline needles when their width is less that one micron (figure 1(c)). In this case, the width of the elongated crystallites is small enough and the crack can cross them. Crystalline needles with widths of several microns act as a barrier to crack propagation (figure 1(d)). In this case, thicker needle-like crystalline inclusions are present where the crack propagated along the periphery and thus is deflected from straight line propagation. In the first case the mode of fracture is transgranular, while in the second is intergranular. In figure 1(d) the radial crack indicated by a white arrow is annihilated by the needle-like crystallite (indicated by a black arrow) that is oriented normal to the propagation direction. In the case of N products we observed needles with widths $\sim$5 μm

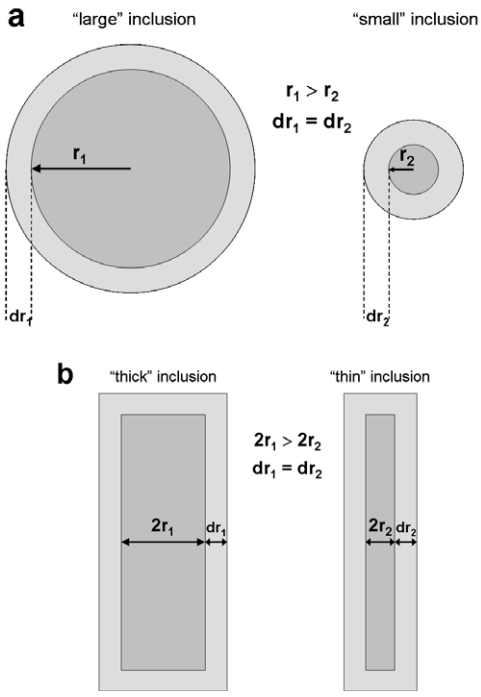

Figure 3. Schematic view of (a) large and small crystalline inclusions represented as circles and (b) needle crystalline inclusions. The light grey regions represent the extent of the interface, while the darker grey regions represent the bulk-like crystallite.

and below 0.5 μm. Needle-like crystallites with intermediate widths were not observed as in the case of G products (figure 2).

4. Discussion

In the present study the crystalline inclusions are dispersed in an amorphous matrix. The crack propagates in the amorphous matrix reaching the interface between the amorphous and the crystalline structure. At the interface region, between the amorphous matrix and crystalline inclusion, the bonding of atoms is different than in the bulk phases. In general, at boundary regions there are atoms with weaker atomic bonding than in the bulk crystallite phases [19].

Thus, the interface region is a region for easier crack propagation, since weaker bonding means that atomic bonds are more easily broken than in the bulk crystallite region. However, another parameter that should be taken into account is the size of the interface as a percentage of the size of the whole crystallite, since the size of the crystallite will affect the bonding of the atoms within the crystallite. In figures 3(a) and (b) two granularly and needle-shaped crystallites are represented schematically as circles and oblong parallelograms, respectively, for simplicity reasons. The lighter grey regions represent the interface regions with the amorphous matrix (white) and the darker grey regions represent the 'bulk' of the crystallites. Note that the thickness of the interface region (dr_i) does not depend on the size of the crystalline inclusion.

In the case of the small crystalline inclusions the ratio of interface area (S_{inter}) over the 'bulk' area of the crystallite (S_{cryst}) is important while in the case of larger crystallites the ratio is reduced. This ratio is an important parameter since once the tip of the crack has reached

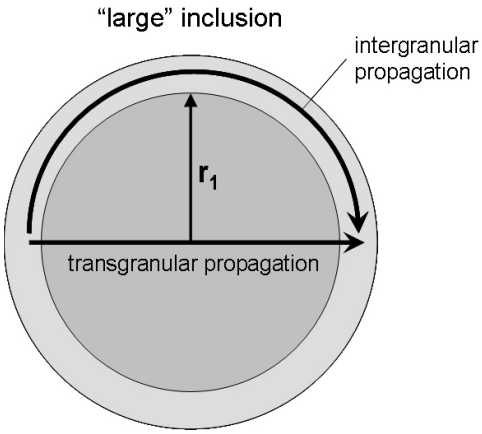

Figure 4. Schematic view of a granular crystallite. Two different paths of the crack are schematically presented. One straight path, corresponding to transgranular propagation through the bulk of the crystallite, and a curved one through the interface region, corresponding to intergranular propagation.

the interface it will have to decide in which direction it will continue i.e. it will go through the crystallite or it will follow a path through the periphery of the crystallite, i.e. through the interface region. In the case of the small crystallites, once the crack has reached the interface and has broken several atomic bonds, a region of nearby atoms in the previously bulk region will be affected and the bonding will get reduced making the propagation through the crystallite also probable (transgranular mode). However, in the case of larger crystallites the bonding of atoms close to the interface will be less affected when the crack will break some bonds and thus the propagation through the interface region will be privileged (intergranular propagation). The above arguments comply with our experimental observations; in the case of crystallites with average size or width smaller than 1 μm (figures 1(a) and (c)) transgranular propagation of the crack is favoured, while for larger crystallites (average size or width of several microns) (figures 1(b) and (d)) either intergranular or blocking of propagation (in the case of elongated crystallites) is monitored.

Having presented the basic assumptions, a detailed analysis will follow, in order to obtain some qualitative results by simple energetic considerations. For simplicity, a circular crystallite is assumed and the energetics of transgranular and intergranular propagation are examined. In the case of crack propagation through the crystallite (transgranular propagation) an amount of energy ($E_{\text{transgranular}}$) is required that is proportional to the characteristic width $2r_1$ of the crystallite (see figure 4):

$$E_{\text{transgranular}} = 2r_1 \times E_{\text{cryst}} \tag{1}$$

where $2r_1$ is the size of the crystallite and E_{cryst} is the bonding energy for the crystallite atoms. In the case that the crack propagates through the interface region between the crystallite and the matrix (intergranular propagation), the energy required ($E_{\text{intergranular}}$) is again proportional to the path

$$E_{\text{intergranular}} = \pi r_1 \times E_{\text{inter}} \tag{2}$$

where E_{inter} is the bonding energy between the atoms at the interface region. In this model it is assumed that the depth of the crack is the same all along the line of crack propagation.

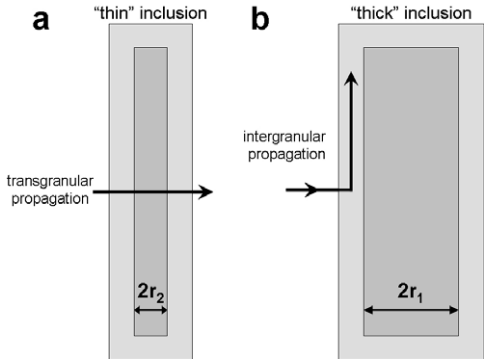

Figure 5. The two modes of fracture for thin (a) and thick (b) needle crystalline inclusions.

Thus, the ratio of energy for intergranular over the energy required for transgranular propagation ($E_{\text{intergranular}}/E_{\text{transgranular}}$) from (1) and (2) is:

$$E_{\text{intergranular}}/E_{\text{transgranular}} = (\pi r_1 E_{\text{inter}})/(2r_1 \times E_{\text{cryst}}) \cong 1.6\, E_{\text{inter}}/E_{\text{cryst}} \tag{3}$$

and it will determine the mode of the crack propagation. In fact, it is the ratio of the bonding energies of atoms in the interface region and the crystallite region ($E_{\text{inter}}/E_{\text{cryst}}$) that will determine the path to be followed. For values of $E_{\text{inter}} \leqslant 0.6E_{\text{cryst}}$ the intergranular propagation is favoured, since in this case $E_{\text{intergranular}} < E_{\text{transgranular}}$. The ratio $E_{\text{inter}}/E_{\text{cryst}}$ will be affected by the size of crystallite since E_{cryst} is expected to increase as a function of crystallite size approaching the bulk value. Thus, as crystallite size increases the intergranular propagation will be favoured. However, we must bear in mind that it will depend also on the chemical composition of the inclusion, since different materials will present different binding and thus the E_{cryst} and E_{inter} and the corresponding ratio $E_{\text{intergranular}}/E_{\text{transgranular}}$ will vary.

The above energetic discussion although qualitative can also explain the morphology of the cracks observed for all products. In the case of small granular crystalline inclusions (figure 1(a)), crack propagation in a straight line is observed, while in the case of larger granular crystalline inclusions (figure 1(b)), intergranular fracture results to a deviation from straight propagation of the crack.

In the case of N product (figure 1(c)), needle crystalline inclusions of various widths are present. For relatively thin needle crystalline inclusions the crack traverses them (transgranular mode) when it hits them in the direction perpendicular to their large side (figure 5(a)). In this case we observe also that when the crack reaches them along their large side it propagates along the interface (intergranular propagation). In the case of relatively thicker needle crystalline inclusions (figure 1(d)), with very large periphery, the crack stops when it reaches the crystallite in the direction perpendicular to its large side (figure 5(b)).

The energetic reasoning seems to explain also, at least qualitatively, the experimental observations about the extent of crack propagation in the case of G product (figure 2) as a function of the crystallite size. An increase in the extent of crack propagation as the size of the crystallites reduces is observed since the smaller size will result in transgranular propagation and thus larger distances travelled by the crack. This is schematically shown in figure 6. In the case of small inclusions (figure 6(a)) the crack propagates passing through the grains (transgranular propagation) and thus the path followed by the crack and the effective distance travelled by the crack, i.e. the length and the extent of the crack, coincide. In the case of large crystallites (figure 6(b)) the crack propagates in intergranular mode, i.e. it follows a path along

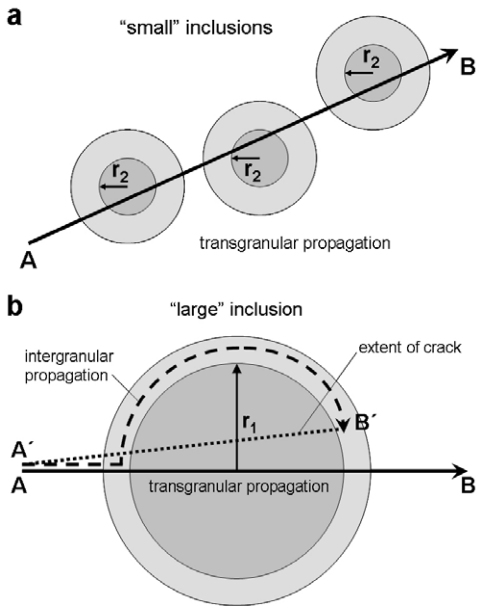

Figure 6. (a) The case of small inclusions, where the crack propagates passing through the grains. The path followed by the crack and the effective distance travelled by the crack coincide. (b) In the case of large crystallite the crack follows a path along the interface (dashed line) and not through the crystallite (straight line) and as a result the extent of crack (the pointed straight line that connects A′ with B′) is shorter than the length of the crack path (dashed line).

the interface (dashed line) and not in transgranular mode (solid line). For comparison reasons the lengths of the solid and dashed lines in figure 6(b) have been drawn equal. However, since the crack follows the intergranular path the effective distance travelled and thus the extent of the crack (represented by the pointed straight line that connects A′ with B′) is shorter than the length of the crack path (dashed line) and consequently shorter than in the case of transgranular propagation.

A question that arises is if there is a characteristic size of crystallites that determine the propagation mode of the crack and as a result the mechanical behaviour of the material under study. A reasonable estimation can be obtained by considering the size at which E_{cryst} will reach a value that will be comparable to the value of a bulk material with the same chemical composition. This will depend on the size of the crystallite in comparison to the interface zone for a two dimensional topology. Since atoms are nearly homogeneously distributed in these regions, a rough estimation will be based on the ratio of the area of interface region (S_{inter}) over the area of bulk crystallite region (S_{cryst}). As a result, as the size of a crystallite increases, E_{inter} will be smaller than E_{cryst} and the crack will preferably follow a path along the interface (intergranular propagation). As the size of the crystallite decreases, E_{cryst} will be closer to E_{inter} and the crack will have an increased probability to cross the crystallite resulting in transgranular propagation.

In the following, a calculation for this ratio in the case of circular crystallites (figure 4) is made. In general, the modified width of the interface extends over several atomic distances. The average size of crystallites ranges from 0.5 μm up to 3 μm, resulting in a radius from 0.25 up to 1.5 μm. Assuming that the interface region is extended over ten interatomic distances, with an average of 5 Å each, the width of the interface is 0.005 μm. It is easy to calculate the

Table 2. Calculated ratio of interface area to bulk crystallite area (S_{inter}/S_{cryst}) for various crystallite sizes, in the case of granular and needle crystallites.

Crystallite size (μm)	Crystallite radius (μm)	Interface width (μm)	S_{inter}/S_{cryst} (%) granular	S_{inter}/S_{cryst} (%) needle
0.2	0.1	0.005	10.00	5.00
0.5	0.25	0.005	4.00	2.00
1.0	0.50	0.005	2.00	1.00
1.5	0.75	0.005	1.33	0.67
2.0	1.00	0.005	1.00	0.50
2.5	1.25	0.005	0.80	0.40
3.0	1.50	0.005	0.67	0.33

ratio of this interface region to the bulk, $S_{inter}/S_{cryst} = 2dr/r$ (table 2). It can be seen that for crystallites of size up to 1.5 μm the ratio is a few per cent and for larger crystallites it falls to less than 1%. It should be mentioned that we consider that the ratio S_{inter}/S_{cryst} equals to the ratio of atoms on the interface over the atoms of the crystallite and its values can be used as an indication of 'bulk' behaviour of the inclusion. For values of S_{inter}/S_{cryst} less than 1% a bulk behaviour is obtained favouring the intergranular propagation.

The calculation is repeated for the case of elongated crystallites. In figure 4(b) it is presented an elongated crystallite of length L and size $2r$ with an interface region of width dr. The ratio in this case is $(2L\,dr + 4r\,dr)/(L2r)$ which for the case of $r \ll L$ simplifies to $S_{inter}/S_{cryst} = dr/r$, very similar to the previous one. The results of these calculations are presented in table 2. Again it is observed that for crystallite sizes over 1–1.5 μm this ratio gets less than 1%. It is of interest that in our work for crystallites with sizes larger than 2–3 μm either intergranular propagation or blocking of propagation occurs (in the case of the elongated crystals). For crystallites of the order of 1–1.5 μm (elongated or not) transgranular propagation occurs.

The decrease of the extent of crack propagation with the increase of mean crystallite size is the result of the shift of fracture mode from transgranular to intergranular. Consequently, increasing the mean crystallite size, a shift from the strengthening towards the toughening effect takes place. This behaviour has been observed in the case of ceramic materials [20], but it has never been reported previously in the case of glass–ceramic materials, according to our knowledge.

The energetic arguments mentioned above can also explain the observed crack propagation extend in the present study in the case of G products. In the case of transgranular propagation (small crystallites) the crack propagates more or less along a straight line while in the case of intergranular propagation it will follow a curved path along the interface of the crystallite with the amorphous matrix. In terms of energy, two cracks with the same energy can break nearly the same number of atomic bonds i.e. a given number of atomic distances. However, in the case of transgranular propagation this happens for bonds in the same direction while in the second case this happens for bonds in a zigzag path. As a result (see figure 4) the effective extent of the crack will be larger in the first case (small crystallites) than in the second case (large crystallites) as it was experimentally observed for the G product (figure 2).

It is of interest to mention here the work of Murashov *et al* [21] on the influence of the Y_2BaCuO_5 particle size distribution on the crack propagation in melt textured YBCO. They have estimated the crack propagation as a function of the size of inclusions and they have found that cracks hitting inclusions smaller than 7 μm were nearly passing through, whereas

crack propagation was almost stopped by inclusions with size exceeding the critical value of 7 μm. The effect of such particles on the toughening of superconducting materials was also studied by Mathieu *et al* [22] who observed that the crack deviates from its initial path when it reached a 211 and tends to propagate around the 211 particle.

The existence of a critical value for the grain size is clear also in our case. This critical size is estimated about 1.5 μm. When the size of the crystallites is larger than this critical size, the crack follows intergranular propagation or it cannot cross the elongated crystals, since the periphery is quite large while in the opposite case it follows transgranular propagation. Thus, it is obvious that by controlling the size and form of crystallites via the devitrification conditions the crack propagation and thus the mechanical properties of the fabricated materials can be significantly affected. However, the nature of the atomic binding of the inclusion atoms should also be taken into account. It should be stressed here that the above limit was found for the specific types of glass–ceramic product and it does not necessarily holds for other types of glass–ceramics, i.e. it is not a universal law. More studies in different compositions and crystallite morphologies are under way in order to observe whether this limit applies.

5. Conclusions

It was experimentally observed that the mean size of the granularly shaped and the width of needle-shaped crystalline inclusions determine the crack propagation mode. For sizes and widths smaller than one micron, transgranular fracture occurs, while for sizes and widths of several microns intergranular fracture occurs. With the help of a physical model the crack propagation mode is related to the ratio of the interface area between the crystalline inclusion and the amorphous matrix over the area of the crystallite inclusion. It turns out that there is a critical value for this ratio that determines the mode of crack propagation. It seems that for a ratio larger than one per cent it is the transgranular propagation that it is favoured while for lower values intergranular propagation or blocking of the crack occurs. This model also explains the behaviour of the length of crack propagation as a function of the size/width of crystalline inclusions.

Acknowledgment

The project is co-funded by the European Social Fund & National Resources-EPEAEK II 'ARCHIMEDES II' programme Sub-Project 2.6.8.

References

[1] Flinders M, Ray D, Anderson A and Cutler R A 2005 *J. Am. Ceram. Soc.* **88** 2217
[2] Zhou Y, Brito M E, Yang J F and Ohji T 2003 *J. Am. Ceram. Soc.* **86** 1789
[3] Sun X, Li J G, Guo S, Xiu Z, Duan K and Hu X Z 2005 *J. Am. Ceram. Soc.* **88** 1536
[4] Strnad Z 1986 *Glass–Ceramic Materials* (New York: Elsevier Science)
[5] Morrell R 1996 *Materials Science and Technology Series* vol 17A, ed R W Cahn, P Haasen and E J Kramer (Weinheim: VCH) p 11
[6] Qin X M, Xiu Z M, Zuo L and Li S 2003 *J. Inorg. Mater.* **18** 1158
[7] Denry I L and Rosenstiel S F 1993 *J. Dent. Res.* **72** 572
[8] Oh W S, Zhang N Z and Anusavice K J 2003 *Int. J. Prosth.* **16** 505
[9] Kim J and Liaw P K 2005 *J. Eng. Mater. Tech. Trans. ASME* **127** 8
[10] Lee S S and Stinchcomb W W 1996 *Key Eng. Mater.* **120** 227
[11] Boccaccini A R, West G and Taplin D M R 1996 *Mater. Sci.* **32** 71
[12] Pagano N J and Brown H W 1993 *Composites* **24** 69

[13] Marshal Y A H 1995 *Eng. Fract. Mech.* **52** 43
[14] Kavouras P, Charitidis C and Karakostas Th 2006 *J. Non-Cryst. Solids* **352** 5515
[15] Kavouras P, Kehagias Th, Tsilika I, Chrissafis K, Kaimakamis G, Papadopoulos D, Kokkou S, Komninou Ph and Karakostas Th 2007 *J. Hazard. Mater.* **139** 424
[16] Kehagias Th, Komninou Ph, Kavouras P, Chrissafis K, Nouet G and Karakostas Th 2006 *J. Eur. Ceram. Soc.* **26** 1141
[17] Kavouras P 2003 Powder processing for the fabrication of advanced materials for technological applications *PhD Thesis* Physics Department, Aristotle University of Thessaloniki
[18] Kavouras P, Komninou Ph and Karakostas Th 2004 *J. Eur. Ceram. Soc.* **24** 2095
[19] Karakasidis T E and Meyer M 1997 *Phys. Rev.* B **55** 13853
[20] Ziegler A, McNaney J M, Hoffmann M J and Ritchie R O 2005 *J. Am. Ceram. Soc.* **88** 1900
[21] Murashov V A, Schätzle P, Krabbes G, Klosowsky J, Wendrock H, Vogel H R and Eversmann K 1996 *Physica* C **261** 181
[22] Mathieu J-P, Cano I G, Koutzarova T, Rulmont A, Vanderbemden Ph, Dew-Hughes D, Ausloos M and Cloots R 2004 *Supercond. Sci. Technol.* **17** 169